1999b
QE-23
289

by Qinghua Huang[1] and Motoji Ikeya[2]

Experimental study on the propagation of seismic electromagnetic signals (SEMS) using a mini-geographic model of the Taiwan Strait

1 International Frontier Program on Earthquake Research, The Institute of Physical and Chemical Research (RIKEN), at Earthquake Prediction Research Center, Tokai University, 3-20-1, Orido, Shimizu 424-8610, Japan; E-mail: huang@iord.u-tokai.ac.jp
2 Department of Earth and Space Sciences, Graduate School of Science, Osaka University, 1-1 Machikaneyama, Toyonaka, Osaka 560-0043, Japan.

Propagation patterns of seismic electromagnetic signals (SEMS) of the 1994 M 7.3 Taiwan Strait earthquake have been simulated experimentally using a geographic model of the Taiwan-Fujian region. The power intensity above a granite slab for electromagnetic (EM) waves transmitted from the source antenna in the slab was mapped. In this model, aluminum foil was used to simulate the ocean and the lower ionosphere and the underground conductive layer were simulated by aluminum plates. The experiment indicated that the EM waves at a frequency higher than the cut-off frequency can propagate in a rippled-pattern, while those at a lower frequency can only be detected in some regions close to geographic boundaries. The variation of the depth and the orientation of the source antenna made little influence, while the distribution of sea and land affected the propagation.

Introduction

The electromagnetic (EM) waves at a broad range of frequencies are reported to have been observed prior to earthquakes (Oike and Ogawa, 1986; Fujinawa and Takahashi, 1990, 1998; Maeda and Tokimasa, 1996; Bella et al., 1998; Molchanov et al., 1998). The so-called seismic electric signals (SES), which are detected in the direct current (DC) electric field, have been used in earthquake prediction in Greece. This approach is known as the VAN (Varotsos, Alexopoulos and Nomicos) method (Varotsos et al., 1996; Uyeda, 1996). However, the method is still controversial (Lighthill, 1996). One of the issues in the controversy is the physical nature of the generation and propagation of SES, although some hypotheses to explain the possible transmission of SES considering the local underground conductivity distribution have been presented (Utada, 1993; Varotsos et al., 1993, 1998).

EM signals were also observed from many rock experiments (Nitsan, 1977; Ogawa et al., 1985; Brady and Rowell, 1986; Cress et al., 1987; Enomoto and Hashimoto, 1990). Some phenomena possibly related with earthquakes, such as lightning, cloud, television noise, anomalous animal behavior and so on, were ascribed to seismic electromagnetic signals (SEMS) (Ikeya and Takaki, 1996; Ikeya and Matsumoto, 1998; Ikeya et al., 1997b; Huang et al., 1997). Recently, an electromagnetic model of a fault, considering the dislocation theory, was developed to explain the possible generation mechanism of EM signals associated with faulting (Huang and Ikeya, 1998b).

It would be necessary to investigate experimentally the propagation of SEMS, till a scientifically credible theory has been made to explain those reported long distance propagation. Motivated by the waveguide concept, a scale-model experiment on the propagation of EM waves in several waveguides has been developed (Ikeya et al., 1997a; Huang and Ikeya, 1998a). Application to two earthquakes in Greece indicated some aspect of long distance propagation of SES (Varotsos et al., 1996) may possibly be related to the distribution of sea and land (Huang and Ikeya, 1998a).

In the present experiment, propagation of EM waves from the *M* 7.3 Taiwan Strait earthquake (September 16, 1994) is investigated using a scale geographic model of the Taiwan-Fujian region. We investigate the possible influences of the depth and the orientation of the source antenna on the propagation pattern of EM waves. In addition, we investigate the influences of the distribution of sea and land and the edge effect of the Earth's crust on the transmission of EM waves.

Experiments

Geographic model

A schematic diagram of the experimental procedures is described in Figure 1a. The Earth's crust (30 km) was simulated by a granite slab (610 mm × 610 mm × 22 mm) with a resistivity of about 10^6 Ωm and a dielectric coefficient, $\varepsilon = 8\varepsilon_0$, where ε_0 is the dielectric coefficient in vacuum. An aluminum plate simulating the conductive boundary in the crust (for simplicity, the Moho plane was assumed in this experiment) was placed against the lower surface of the granite slab. Another aluminum plate at 44 mm above the upper surface of the granite slab simulated the lower ionosphere at 60 km above the ground surface. The Taiwan-Fujian region was modeled in a scale of 1 : 1,360,000 and the conductive sea surface was covered with aluminum foil (Figure 1b). The model hypocenter was fixed in a hole drilled at the center of the bottom of the granite slab. The EM signals associated with the 1994 *M* 7.3 Taiwan Strait earthquake was simulated by emission of microwaves from a loop antenna placed at the model hypocenter.

Experimental apparatus

EM waves were emitted from a one-turn loop antenna placed at the hypocenter connected with a microwave synthesizer with varied frequency. The detector was another loop antenna, placed close to the surface of the granite slab. It scanned over the surface by an *X-Y* plotter and the output was connected to a spectrum analyzer. Directions of both antennas were changed so that the loop could be in a

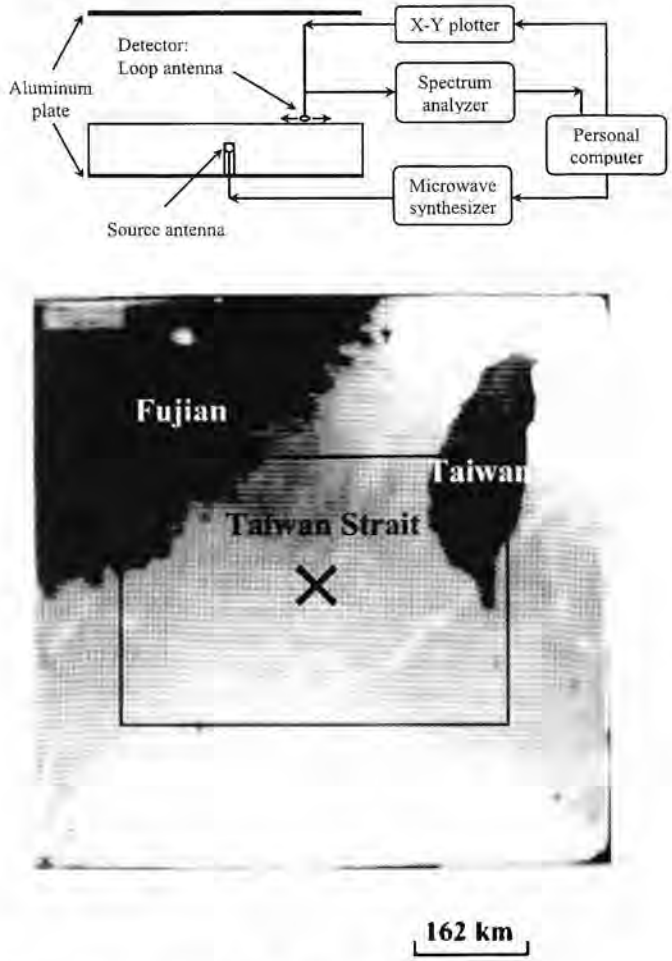

Figure 1 (a) A schematic diagram of the experimental procedures on the propagation of electromagnetic waves (above). (b) A photo of the geographic model of the Taiwan region. The cross is the model epicenter. The rectangular box indicates the experimentally investigated region of 400 mm × 280 mm. The size of the granite rock is 610 mm × 610 mm. The bright zone is covered by aluminum foil simulating the ocean and dark zone represents the land (below).

horizontal plane and a vertical plane. The scanned area was 400 mm × 280 mm (Figure 1b). The microwave synthesizer, *X-Y* plotter and spectrum analyzer were all controlled by a personal computer and the data were processed to make a map of power intensity distribution of EM waves.

The EM waves at two frequencies of 158 MHz and 1.58 GHz corresponding to frequencies of 116 Hz and 1.16 kHz in the real earth (conversion is based on, $f_r \bullet \lambda_r = f_m \bullet \lambda_m = c$, where suffix r and m represent real case and model, c is light velocity.) were used to examine the frequency dependence of propagation, considering the scale of the geographic model. In this paper, we note quantities in the real case in the bracket after the model quantities, e.g., 158 MHz (116 Hz), etc. The power intensity of the source was fixed at 15 dBm (0.0316 W). Note that dBm is the unit of power used in this study, which is defined as 10 times of the logarithm of the power in unit of 10^{-3} W, i. e., Power (dBm) = 10 $\log_{10}$ Power (10^{-3} W).

Waveguide model

Generally, waveguide can be defined as a system of at least two media, separated by at least one dividing surface, where wave is guided. There are many kinds of waveguide due to different nature of media. The simplest type would be a waveguide consists of two perfectly conductive parallel plates between which EM waves are trapped and guided. This type of waveguide is called as "parallel-plate waveguide".

One may find the detailed discussions in literatures (e.g., Reitz and Milford, 1967; Waldron, 1970; Staelin et al., 1994). Here we only show that there is a cut-off frequency f_c of parallel-plate waveguide with $f_c = c^*/2d$, where c^* is wave velocity in the medium ($c^* = 1/(\varepsilon\mu)^{1/2}$ using dielectric coefficient ε and permeability μ of the medium) and d is the separation distance between two palates of the waveguide. Waves at a frequency $f < f_c$ will be exponentially damped, instead of propagating in case of $f > f_c$. That is why f_c is called as "cut-off" frequency. The reason why waves at $f < f_c$ are damped can be explained as follows.

For simplicity, waves are assumed to propagate along z-axis (Figure 2). Then, the propagation in the parallel-plate waveguide can be described in terms of the exponential factor, e.g., $\exp(jk_z z)$, where k_z is the wave-number along the z direction. The guided condition for the simplest mode gives $k_z = 2\pi((f/c^*)^2 - (1/2d)^2)^{1/2}$ (e.g., Staelin et al., 1994). The cut-off frequency f_c is obtained as $f_c = c^*/2d$ from $k_z = 0$ (corresponding to the incidence angle, $\theta = 0$ in Figure 2). Then, one can obtain $k_z = 2\pi((f/c^*)^2 - (1/2d)^2)^{1/2} = \pi/d((f/f_c)^2 - 1)^{1/2}$, after substituting $c^* = 2d \bullet f_c$ into k_z. Therefore, an imaginary coefficient (wave-number, k_z) in propagating will appear when $f < f_c$. Namely, wave is damped rather than oscillating.

The EM waves are assumed to propagate within the following three parallel plate waveguides: (1) ionosphere-ocean, (2) ocean-conductive boundary in the crust, and (3) ionosphere-conductive boundary in the crust.

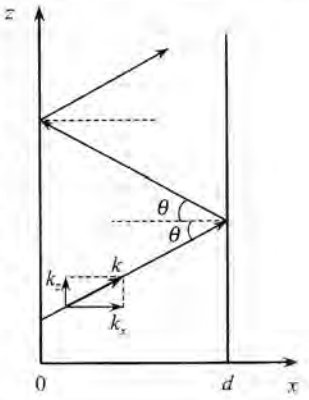

Figure 2 A parallel-plate waveguide model with a separation distance of d. Waves are assumed to propagate along the z direction, e.g. in terms of exp(jk$_z$z), where k$_z$ is the wave number along the z direction. The incidence angle θ = 0 and k$_z$ = 0 at the cut-off frequency f$_c$ = c*/2d, which means waves bounce at the same place along the x direction without propagating along the z direction.

Results and discussions

The EM waves would propagate in the three possible earth-waveguides having different cut-off frequencies. For simplicity, we only estimate the cut-off frequency using the parallel-plate waveguide model. The ionosphere-crust waveguide model leads to $f_{c1} = c/\lambda_{c1} = c/2d = 2.27$ GHz, which corresponds to 1.67 kHz in the real case, using the light velocity $c = 3\times10^8$ m s^{-1} ($c = 1/(\varepsilon_0\mu_0)^{1/2}$ using dielectric coefficient ε_0 and permeability μ_0 in vacuum) and distance between the ionosphere and the Moho plane $d = 66$ mm (9×10^4 m). However, our waveguide model is equivalent to a real waveguide containing two different media (e.g., crust and air). Therefore, the cut-off frequency should be less than the above estimated value, i.e., $f_{c1} < 2.27$ GHz (1.67 kHz). If the dielectric coefficient of the crust is assumed as $\varepsilon = 8\varepsilon_0$, then a tentative estimation of the cut-off frequency considering an average velocity of EM waves (media discussed here are non-magnetic, i.e., $\mu = \mu_0$, so $c^* = c/(\varepsilon/\varepsilon_0)^{1/2}$) in this waveguide would lead to $f_{c1} = 1.41$ GHz (1.04 kHz) (see Table 1). The cut-off frequencies of the ionosphere-ocean waveguide and the ocean-crust waveguide would be $f_{c2} = 3.41$ GHz (2.50 kHz) and $f_{c3} = 2.41$ GHz (1.77 kHz), respectively as summarized in Table 1.

Table 1 Dimensions (separation distance of two parallel planes: d) and cut-off frequencies (f_c) of three waveguides, where f_c is estimated simply from $f_c = c^*/2d$ using the velocity of electromagnetic waves in the medium c^*, where $c^* = c/(\varepsilon/\varepsilon_0)^{1/2}$ using the velocity in vacuum c, the dielectric coefficient ε in the medium ($\varepsilon = 8\varepsilon_0$ for the crust and $\varepsilon = \varepsilon_0$ for air) and ε_0 in vacuum.

Waveguide	Ionosphere-crust	Ionosphere-ocean	Ocean-crust
Separation distance d (km)	90	60	30
Cut-off frequency f_c (kHz)	< 1.67 (1.04)*	2.5	1.77
Experimental separation d_{exp} (mm)	66	44	22
Experimental cut-off frequency f_{exp} (GHz)	< 2.27 (1.41)*	3.41	2.41

* The number in the bracket is a tentative estimation of cut-off frequency considering an average speed of electromagnetic waves in the ionosphere-crust waveguide model.

Note that the height of the lower ionosphere layer is assumed as 60 km in this study. If the height is taken as 120 km (at night), a lower cut-off frequency than above estimations (in the cases of the ionosphere-crust and the ionosphere-ocean waveguides) would be obtained.

The main experimental results are summarized in Table 2.

Effect of the distribution of sea and land to the propagation of EM waves

Figure 3(a) indicates that the EM waves are undetectable except at some geographic boundaries at 158 MHz (116 Hz) which is lower than the cut-off frequency, e.g., f_{c1}. More intense EM waves with a rippled propagation pattern were observed as shown in Figure 3(b) at 1.58 GHz (1.16 kHz) which is higher than the cut-off frequency.

Simple parallel-plate waveguide model predicts that the intensity of EM waves at a frequency lower than the cut-off frequency should decay exponentially from the source. However, no obvious decay pattern (see Figure 3(a)) was obtained in our experiment at the low frequency of 158 MHz (116 Hz). This is considered to be due to the reflection effect of the aluminum foil which simulated the large ocean region.

We made a similar experiment after removing the aluminum foil from the ocean part to investigate the ocean influence on the

Table 2 The experimental results of EM waves associated with the M 7.3 Taiwan Strait earthquake (September 16, 1994) at two frequencies which are lower and higher than the cut-off frequency of earth-waveguide. The numbers in the bracket represent the quantities for the real earth. Al: aluminum. SES: seismic electric signals.

Frequency		158 MHz (116Hz) ($f < f_c$)	1.58 MHz (1.16 kHz) ($f > f_c$)	Remarks
Ocean effect	With the ocean area covered by Al foil	Signals only appear in the regions close to geographic boundaries (Figure 3a).	Disturbed rippled pattern (Figure 3b)	Appearance of the broad ocean not only disturbed the rippled pattern at a high frequency, but also led to a complete different pattern at a low frequency, which may provide a partial explanation for the selectivity of SES.
	Without the ocean zone covered by Al foil	Exponential decay from the model epicenter (Figure 3c).	Rippled pattern (Figure 3d)	
Source effect	Shallow 7.3 mm (10 km)	Signals appear around geographic boundaries (Figure 3a).	Disturbed rippled pattern (Figure 3b)	Signals at a low frequency are very weak if the source is at a deep site. Source depth does not influence the propagation pattern of EM waves.
	Deep 16.1 mm (22 km)	Similar pattern as above with relative weak signals.	Similar pattern as above results	
Effect of the source antenna	Vertical orientation	Signals appear in the regions close to geographic boundaries.	Disturbed rippled pattern (Figure 3b)	Vertical orientation of the source antenna enhances the signal intensity a little at a low frequency. Orientation of the source loop antenna made little influence on the propagation.
	Horizontal orientation	Similar to Figure 3a with relative weak intensity.	Rippled pattern almost the same as above	
Edge effect	With conductive side edges of granite slab (crust)	Signals appear only in the regions close to geographic boundaries (Figure 4a).	Disturbed rippled pattern (Figure 4b)	Reflection of conductive edges enhances the signal intensity at a low frequency. Reflection from edges also influence the propagation pattern at a high frequency.
	Without conductive side edges	Similar pattern with relative weak intensity.	Rippled pattern slightly modified.	

propagation of EM waves. Figure 3c is the experimental intensity distribution of EM waves at a frequency of 158 MHz (116 Hz). The EM waves decayed exponentially, which is completely different from the result shown in Figure 3a. No signals can be detected over a long distance from the model epicenter.

The intensity map of EM waves at 1.58 GHz (1.16 kHz) without aluminum foil over the ocean is shown in Figure 3d. An obvious rippled propagation pattern is obtained in this case. This propagation pattern is disturbed when the ocean area is covered by the aluminum foil as shown in Figure 3b.

Effect of the depth of the source antenna to the propagation of EM waves

We have made two experiments with the source at a shallower position, e.g., 7.3 mm (10 km) (Experiment S: Shallow source), and at the model hypocenter, i. e., 16.1 mm (22 km) (Experiment D: Deep source), respectively.

Experiment S: The power intensity maps of EM waves at a low frequency and a high frequency were obtained as shown in Figure 3a and 3b as discussed already.

Experiment D: The propagation pattern of EM waves at 158 MHz (116 Hz) is similar to that of Figure 3a. However, the intensity for the deep source is much lower than that of the shallow one. The intensity map of EM waves at 1.58 GHz (1.16 kHz) is almost the same as Figure 3b.

These results indicated that the intensity of the EM waves at a frequency lower than the cut-off frequency would be much weaker if the source is at a deeper site. However, the propagation patterns are similar.

The wavelength of EM waves might be roughly estimated from the rippled-pattern of the experimental results, i.e., the approximate half waveguide-wavelength would be equivalent to the distance between the rippled-lines. Therefore, the waveguide-wavelength 260~360 km obtained from Figure 3b would correspond to f = 1250~833 Hz with an average of about 1.04 kHz, which is close to the frequency of the source EM waves (1.16 kHz in the real earth). One at least can conclude from the experiments that the cut-off frequency would be lower than 1.04 kHz in this complicated waveguide.

Effect of the orientation of the source antenna to the propagation of EM waves

All previous power intensity maps of EM waves were obtained for the case where the source loop antenna was placed in a vertical plane. Similar experiments have been done to investigate the effect of changes of the orientation of the source antenna from a vertical plane to a horizontal plane. Almost the same propagation patterns as seen in Figures 3a and 3b were observed at both frequencies, except a little difference in the power intensity. Therefore, we may conclude that the orientation of the source antenna would not have much influence on the propagation pattern of EM waves.

Effect of the edge reflection to the propagation of EM waves

Ideally, the crust should be continuous horizontally. If the surface area of the granite slab is much larger than the scanned region, the edge effect on the propagation of EM waves would be negligible. However, the size of the granite slab is only 610 mm×610 mm due to the experimental constraints, while the scanned region is 400 mm× 280 mm (Figure 1b). Therefore, there might be some edge effect to the propagation of EM waves in our experiment. In nature, the conductive fault plane or subduction zone might act as conductive edges.

We have made the experiments with the four side edges of the granite slab wrapped by aluminum foil to investigate the effect of the edge reflection. Figure 4a is the intensity distribution of EM waves at 158 MHz (116 Hz), which is lower than the cut-off frequency. Comparing with the result of Figure 3a, we can at least conclude that the intensity of EM waves tend to become more intense due to the edge reflection.

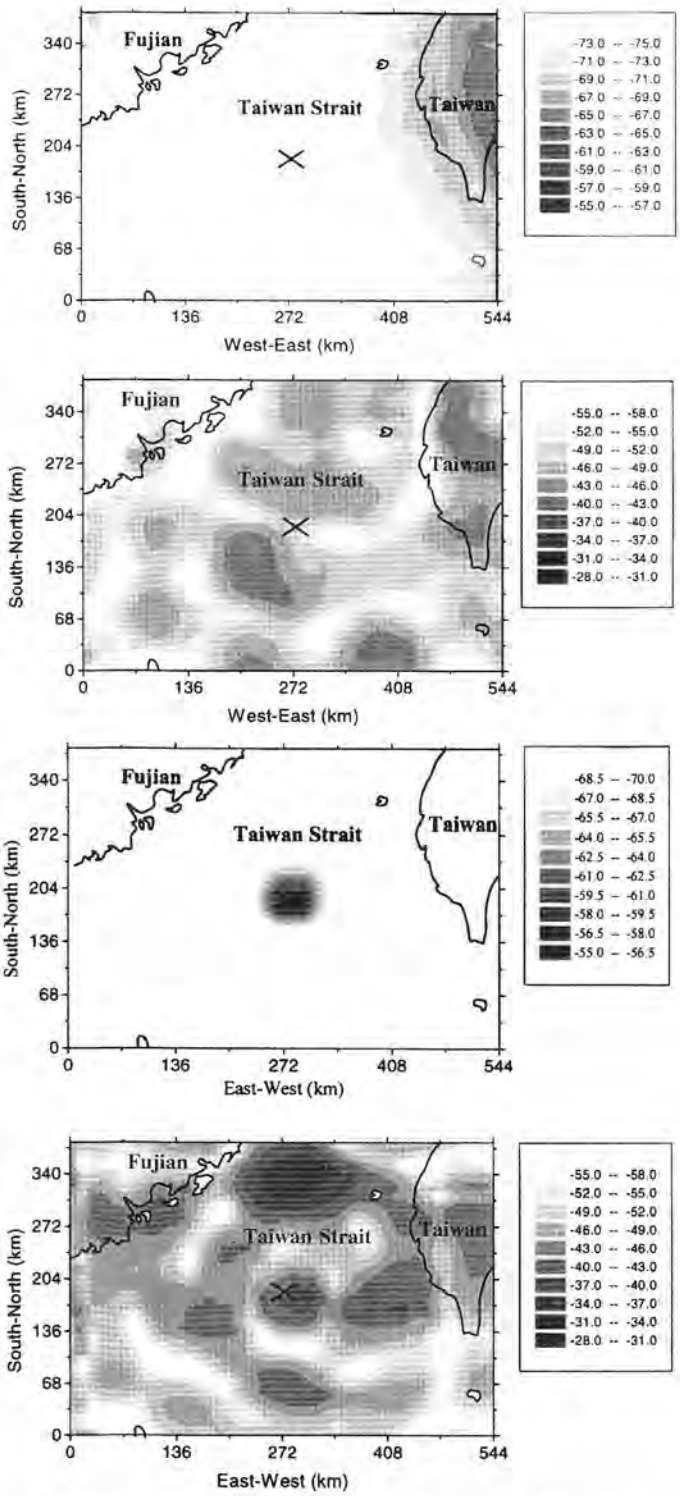

Figure 3 Power intensity maps of EM waves on the surface of granite slab. Power intensity is in unit of dBm, which satisfies Power (dBm) = 10 $\log_{10}$ Power (10^{-3} W). From top to bottom: (a) and (b) are the cases at 158 MHz (116 Hz) and 1.58 GHz (1.16 kHz) with the ocean covered by aluminum foil. (c) and (d) are the cases corresponding to (a) and (b) after removing aluminum foil from the ocean area.

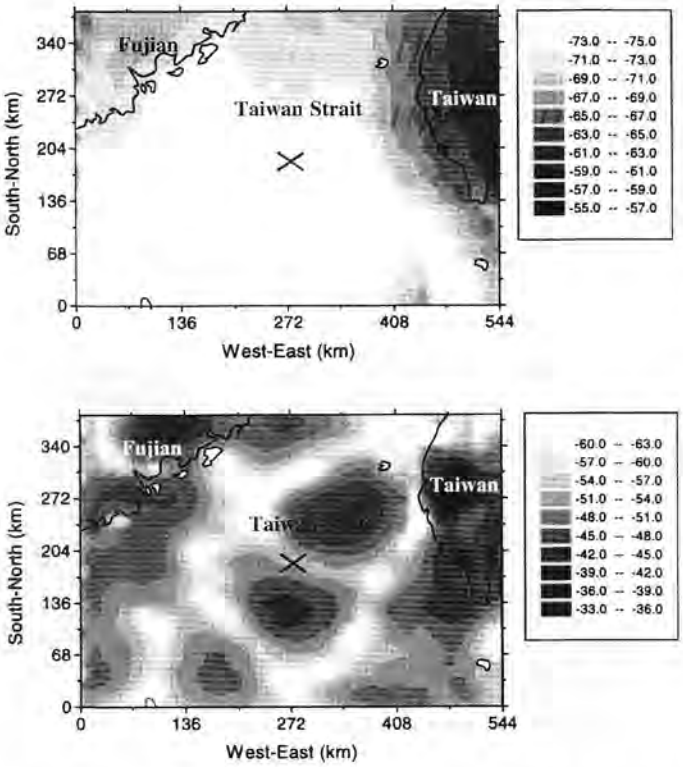

Figure 4 Power intensity maps of EM waves with the side edges of the granite slab wrapped by aluminum foil. From top to bottom: (a) At 158 MHz (116 Hz). (b) At 1.58 GHz (1.16 kHz).

The experimental result of EM waves at 1.58 GHz (1.16 kHz) was obtained as shown in Figure 4b. Even though a rippled propagation pattern was obtained, one may find that the present pattern is different from the previous one without the edge wrapped by aluminum foil (Figure 3b). It seems that the propagation pattern of EM waves is disturbed by the reflection of the conductive edge (aluminum foil). This indicates that fault plane or subduction zone, which may be conductive, may affect the general reflection pattern of EM waves.

Our previous experiments of the Greek archipelago indicated that the ocean effect was not obvious enough if the source is in the main land. Some disturbance to the propagation appeared when the source is close to a geographic boundary, e.g., the Korinthiakos Kolpos bay in the central Greece (Huang and Ikeya, 1998a). In our present experiments, the source is in the ocean. Therefore, the broad ocean zone would play an important role in influencing the propagation of EM waves. This was confirmed by our experimental results (Figures 3a and 3c, 3b and 3d). Observations of SEMS should be made taking these simulations into consideration.

Conclusions

A waveguide model experiment was performed to investigate the propagation characteristics of EM waves, taking, as an example, the geography of the Taiwan-Fujian region with the ocean part covered by aluminum foil. The EM waves at a frequency lower than the cut-off frequency can only be detected close to geographic boundaries. The EM waves higher than the cut-off frequency showed a roughly rippled pattern of propagation. The conductive ocean influenced the propagation patterns. The source depth and the orientation of the source antenna made little influence on the propagation of EM waves, while the effect of the aluminum edge was found somewhat significant.

Acknowledgments

We thank Dr. T. Yamanaka, K. Kinoshita, R. Ikuta, K. Teramoto, Dr. T. Takaki and H. Matsumoto for the help of the experiment and useful discussions. The authors also thank Prof. S. Uyeda for his critical review and insightful suggestion.

References

Bella F., Biagi P.F., Caputo M., Cozzi E., Della Monica G., Ermini A., Plastino W. and Sgrigna V., 1998. Field strength variations of LF radio waves prior to earthquakes in central Italy. Physics of The Earth and Planetary Interior, 105, pp. 279-286.

Brady B. T. and Rowell G. A., 1986. Laboratory investigation of the electrodynamics of rock fracture. Nature, 321, pp. 488-492.

Cress G. O., Brady B. T. and Rowell G. A., 1987. Sources of electromagnetic radiation from fracture of rock samples in the laboratory. Geophysical Research Letters, 14, pp. 331-334.

Enomoto Y. and Hashimoto H., 1990. Emission of charged particles from indentation fracture of rocks. Nature, 346, pp. 641-643.

Fujinawa Y. and Takahashi K., 1990. Emission of electromagnetic radiation preceding the Ito seismic swarm of 1989. Nature, 347, pp. 376-378.

Fujinawa Y. and Takahashi K., 1998. Electromagnetic radiations associated with major earthquakes. Physics of The Earth and Planetary Interior, 105, pp. 249-259.

Huang Q. and Ikeya M., 1998a. Seismic electromagnetic signals (SEMS) explained by a simulation experiment using electromagnetic waves. Physics of The Earth and Planetary Interior, 109, pp. 107-114.

Huang Q. and Ikeya M., 1998b. Theoretical investigation of seismic electric field associated with faulting. Earthquake Research in China, 12, pp. 295-302.

Huang Q., Ikeya M. and Huang P., 1997. Electric field effects on animals: mechanism of seismic anomalous animal behaviors (SAABs). Earthquake Research in China, 11, pp. 109-118

Ikeya M. and Takaki S., 1996. Electromagnetic fault for earthquake lightning. Japan Journal of Applied Physics, 35, pp. L355-L357.

Ikeya M. and Matsumoto H., 1998. Duplicated earthquake precursor anomalies of electric appliances. South China Journal of Seismology, 18 (2), pp. 53-57.

Ikeya M., Kinoshita Y., Matsumoto H., Takaki S. and Yamanaka C., 1997a. A model experiment of electromagnetic wave propagation over long distances using waveguide terminology. Japan Journal of Applied Physics, 36, pp. L1558-L1561.

Ikeya M., Sasaoka H., Teramoto K. and Huang Q., 1997b. Ferroelectric alignment of piezo-compensating quasi-dipolar charges and formation of tornado-like earthquake could. Ionics, 23 Supplement 2, pp. 3-11.

Lighthill S. J. (ed.), 1996. A Critical Review of VAN: Earthquake Prediction from Seismic Electrical Signals, World Scientific Press, Singapore, 376 pp.

Maeda K. and Tokimasa N., 1996. Decametric radiation at the time of the Hyogo-ken Nanbu earthquake near Kobe in 1995. Geophysical Research Letters, 23, pp. 2433-2436.

Molchanov O.A., Hayakawa M., Oudoh T. and Kawai E., 1998. Precursory effects in the subionospheric VLF signals for the Kobe earthquake. Physics of The Earth and Planetary Interior, 105, pp. 239-248.

Nitsan U., 1977. Electromagnetic emission accompanying fracture of quartz-bearing rocks. Geophysical Research Letters, 4, pp. 333-336.

Ogawa T., Oike K. and Miura T., 1985. Electromagnetic radiations from rocks. Journal of Geophysical Research, 90, pp. 6245-6249.

Oike K. and Ogawa T., 1986. Electromagnetic radiations from shallow earthquakes observed in the LF range. Journal of Geomagnetism and Geoelectricity, 38, pp. 1031-1040.

Reitz J. R. and Milford F. J., 1967. Foundations of Electromagnetic Theory, Addison-Wesley, 435 pp.

Staelin D. H., Morgenthaler A. W. and Kong J. A., 1994. Electromagnetic Waves, Prentice-Hall International Inc., Tokyo, 562 pp.

Utada H., 1993. On the physical background of the VAN earthquake prediction method. In: Measurement and Theoretical Models of the Earthis Electric Field Variations Related to Earthquakes (Edited by Varotsos P. and Kulhanek O.). Tectonophysics, 224, pp. 153-160.

Uyeda S., 1996. Introduction to the VAN method of earthquake prediction. In: A Critical Review of VAN: Earthquake Prediction from Seismic Electrical Signals (Edited by Lighthill S. J.), pp. 3-28, World Scientific Press, Singapore.

Varotsos P., Alexopoulos K. and Lazaridou M., 1993. Latest aspects of earthquake prediction in Greece based on seismic electric signals, II. In: Measurement and Theoretical Models of the Earthís Electric Field Variations Related to Earthquakes (Edited by Varotsos P. and Kulhanek O.). Tectonophysics, 224, pp. 1-37.

Varotsos P., Lazaridou M., Eftaxias K., Antonopoulos G., Makris J. and Kopanas J., 1996. Short term earthquake prediction in Greece by seismic electric signals. In: A Critical Review of VAN: Earthquake Prediction from Seismic Electrical Signals (Edited by Lighthill S. J.), pp. 29-76, World Scientific Press, Singapore.

Varotsos P., Sarlis N., Lazaridou M. and Kapiris P., 1998. Transmission of stress induced electric signals. Journal of Applied Physics, 83, pp. 60-70.

Waldron R. A., 1970. Theory of Guided Electromagnetic waves, Van Nostrand Reinhold Company, London, 520 pp.

***Qinghua Huang**, Ph D, graduated from the University of Science and Technology of China in 1990, obtained a Master degree from the Institute of Seismology, China Seismological Bureau in 1993 and awarded Ph D by Osaka University in 1999. He has been a visiting researcher in Kobe University. Now he is a researcher of the International Frontier Program on Earthquake Research, the Institute of Physical and Chemical Research (RIKEN). Research interests include geoelectromagnetism (model, observation and data processing), engineering seismology, strong ground motion and disaster prevention.*

***Motoji Ikeya**, graduated from Department of Electronics Engineering, Osaka University in 1963 and obtained PhD in Nuclear Engineering. Research associate in Physics Department, University of North Carolina and fellow of the Humbodt Foundation from 1976-1978 at University of Stuttgart. Professor of Osaka University in Department of Physics in 1987 and of Earth and Space Sciences since 1991. His research interests include electron spin resonance (ESR) dating, physics of seismic precursors, and seismic electromagnetism.*

Episodes is your window to the world. Subscribe today!

Episodes

Name_____(please print)

Address _____

City _____ State/Prov._____

Country _____Zip/Postal Code_____

Please begin my subscription:

March	June	Sept.	Dec.
____ Year	____Year	____ Year	____ Year

To start your subscription, fill in this form and mail to:

Episodes
P.O. Box 823
26 Baiwanzhuang Rd.,
Beijing 100037, China
Tel: +86-10-6832 0827; +86-10-6832 7772
Fax: +86-10-6832 8928
E-mail:episodes@public2.bta.net.cn

Payment may be made by:

- Checks (US $ only) made payable to *Episodes*
- ❑ Diners ❑ JCB ❑ Visa
  ❑ American Express ❑ Mastercard

Please quote account number, expiry date and signature.

Account# | | | | | | | | | | | | | | | | |

Expiry date_____

Signature _____

Annual subscription rates: US$ 24